Brillouin scattering study of gallium nitride: elastic stiffness constants

1997 J. Phys.: Condens. Matter 9 241

(http://iopscience.iop.org/0953-8984/9/1/025)

J. Phys.: Condens. Matter **9** (1997) 241–248. Printed in the UK PII: S0953-8984(97)74522-3

Brillouin scattering study of gallium nitride: elastic stiffness constants

M Yamaguchi†, T Yagi‡, T Azuhata§, T Sota§, K Suzuki§, S Chichibu‖ and S Nakamura¶

† Department of Applied Physics, Faculty of Engineering, Hokkaido University, 060 Sapporo, Japan

‡ Research Institute for Electronic Science, Hokkaido University, Sapporo 060, Japan

§ Department of Electrical, Electronics and Computer Engineering, Waseda University, Shinjuku, 169 Tokyo, Japan

‖ Faculty of Science and Technology, Science University of Tokyo, 278 Chiba, Japan

¶ Department of Research and Development, Nichia Chemical Industries Ltd., Anan, 774 Tokushima, Japan

Received 15 May 1996, in final form 13 September 1996

Abstract. High-resolution Brillouin scattering measurements on a high-quality wurtzite gallium nitride (GaN) single crystal were carried out and elastic stiffness constants were determined.

A comparison is given with the results of a recently reported model for calculation of the elastic constants of III–V semiconductors based on the modified version of Keyes's relations. A good agreement is found between the experimental and theoretical elastic constants for GaN.

1. Introduction

Gallium nitride is one of the major semiconductors that have been under extensive theoretical and experimental investigation over the past few years [1–4]. Continuous progress in the development of new electronic and optoelectronic devices based on the physical properties of III–V semiconductors has intensified effort for both improving materials processing techniques and understanding their physical and chemical properties [5–8].

A great number of theoretical studies have been made in recent years ranging from empirical to *ab-initio* techniques in order to study the elastic properties of III–V semiconductors [9–12]. However, in many cases there are still no experimental data available for enlightening discussion, largely owing to the difficulties of growing high-quality crystals. Recent success in the growth of high-quality single-crystal gallium nitride on a sapphire substrate by the two-flow MOCVD method has been achieved by Nakamura *et al* [5]. All symmetry-allowed optical phonons for GaN have been observed by Raman scattering from the sample, indicating the high quality of the GaN crystal [13]. In the present work we have performed Brillouin scattering from this sample to determine the elastic stiffness constants. The high-resolution Brillouin scattering technique is a reliable and extremely powerful tool which allows accurate determination of the elastic constants [14, 15]. Recently, a new model has been proposed for the calculation of the elastic constants of III–V compounds and theoretical values of the elastic constants have been presented for both cubic zincblende (ZB) and hexagonal wurtzite (WZ) structures [16]. A comparison of theoretical and experimental elastic constants of hexagonal GaN will be given here.

0953-8984/97/010241+08$19.50

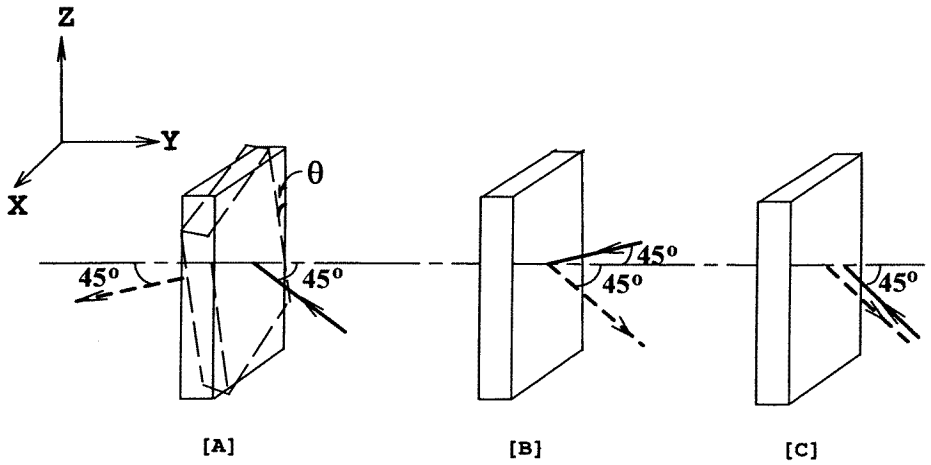

Figure 1. Brillouin scattering geometries used in this work. The horizontal line shows the direction of the c axis. The solid line indicates the direction of incident light and the broken line indicates the direction of scattered light. In geometry [A] the wave vector $\boldsymbol{Q}$ is perpendicular to the c axis. θ is the orientation angle formed between the z axis and the crystal edge when the sample is rotated around the c axis. In geometry [B] $\boldsymbol{Q}$ is parallel to the c axis. Geometry [C] is the 180° scattering geometry.

2. Experimental details

A high-quality single-crystal GaN film was grown on the sapphire substrate using the two-flow MOCVD technique. A detailed description of crystal growth and quality of the sample has been given in [5, 7]. We used a Sandercock-type six-pass tandem Fabry–Perot interferometer (finesse 50) as a spectrometer in our Brillouin scattering system. An Ar^+ ion laser operated at $\lambda = 514.5$ nm with a longitudinal single mode used as the light source. The average incident light power was 100 mW. Brillouin scattering spectra were recorded with a multichannel scaler with 1024 channels and were accumulated 2000–3000 times with a 0.5 s/channel scan.

3. Results and discussion

The sample used in the Brillouin scattering measurements reported here was a GaN single crystal 4 μm in thickness epitaxially grown on a sapphire (0001) substrate. The c axis of GaN is parallel to the c axis of the sapphire substrate. This 4 μm thickness of the sample gives too small a scattering volume compared with the aperture of the pinholes used in our experimental system (200 μm). In order to distinguish clearly Brillouin modes arising from scattering from GaN and those from the substrate, we performed Brillouin scattering measurements of both GaN on a sapphire substrate, and a sapphire substrate without GaN layer. By comparing the two spectra with the help of the peak-fitting analysis, we succeeded in assigning Brillouin peaks unambiguously. The scattering geometries employed in this work are summarized in figure 1.

The Brillouin spectra of GaN on a sapphire substrate and the spectra of the sapphire substrate itself are shown in figures 2(a) and 2(b), respectively. Spectra were taken in the right-angle scattering geometry where the wave vector $\boldsymbol{Q}$ of the acoustic phonon is on

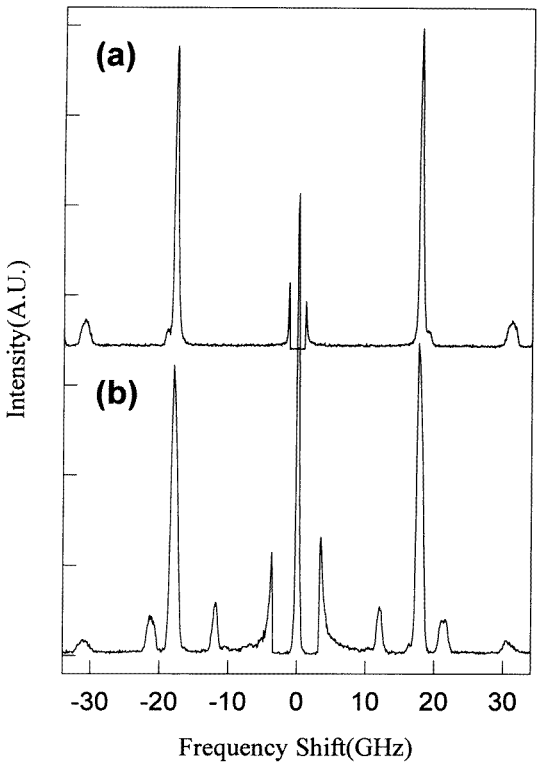

Figure 2. Brillouin spectra of (a) the sapphire substrate and (b) GaN on the sapphire substrate in geometry [A] with V − V + H polarization.

the c plane and the X–Y plane was chosen as a scattering plane, as shown by geometry [A] in figure 1. The polarizations of incident and scattered lights were V and V + H, respectively, where V and H refer to the polarizations of light perpendicular and parallel to the scattering plane. Two additional peaks—near 12 and 21 GHz—are observed in figure 2(b), compared with figure 2(a), as a result of scattering from GaN. To check the polarization of the peaks, Brillouin spectra were observed with different polarizations of incident and scattered lights (H − H in figure 3(a) and H − H + V in figure 3(b)). The peaks which have the same frequency shifts in figures 3(b) and 2(b) are of the same origin, although the relative intensities of the peaks are different in those spectra due to the different elements of Pockel's elasto-optic tensor responsible for each spectrum. In figure 3(a), peaks near 12 and 19 GHz disappear entirely, which indicates that those peaks are depolarized, while other peaks are polarized. From these considerations, we can conclude that the peaks near 12 and 21 GHz are the GaN depolarized and polarized peaks, respectively.

GaN has a hexagonal structure with the space group C_{6v}^4. Acoustic phonons propagating in the c plane correspond to the elastic constants c_{11}, c_{44} and c_{66}. The scattering intensity of the shear c_{44} mode is zero in the present scattering geometry, and the longitudinal c_{11} and shear c_{66} modes have non-zero scattering intensities and are expected to exhibit polarized and depolarized peaks, respectively. From these results, the peaks near 21 and 12 GHz in figure 2(b) were assigned to c_{11} and c_{66} modes, respectively.

Next, we measured the Brillouin spectra while changing the direction of the $\boldsymbol{Q}$-vector

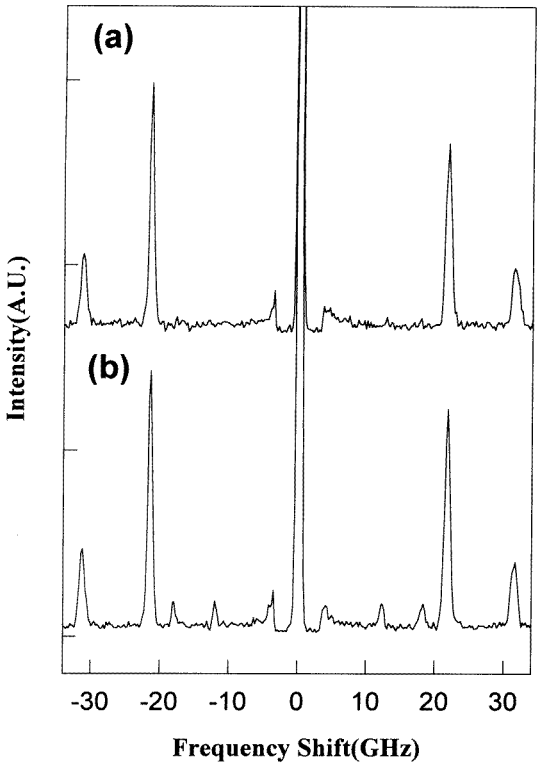

Figure 3. Brillouin spectra of GaN on the sapphire substrate in geometry [A] with (a) H − V and (b) H − H + V polarization.

in c plane. Figure 4 shows the dependence of frequency shifts on the orientation angle θ defined in figure 1, geometry [A]. As shown in figure 4, peaks near 12 and 21 GHz have constant frequency shifts independent of θ, while other peaks have shifts dependent on θ, as expected for sapphire which has a rhombohedral structure with the space group D^6_{3d}. Forbidden by the selection rules for this scattering geometry in the hexagonal structure, the c_{44} mode of GaN was not observed. The frequency shift is constant in the c plane for GaN peaks (figure 4).

Now we consider the acoustic wave propagating in the direction parallel to the c axis. In this direction, there are two modes: the c_{33} longitudinal acoustic mode and doubly degenerate c_{44} shear acoustic mode for both the sapphire substrate and GaN. The scattering geometry was chosen as geometry [B] in figure 1. The Brillouin spectra of GaN on the sapphire substrate and the substrate itself are shown in figures 5(a) and 5(b), respectively. The Brillouin spectrum exhibits a depolarized peak near 38 GHz and a polarized peak near 70 GHz in both figures 5(a) and 5(b). The peaks shown in figure 5(b) have a sharp Lorentzian shape compared with figure 5(a). From polarization selection rules, these peaks can be assigned to to c_{44} and c_{33} modes, respectively, of the sapphire substrate. The Brillouin peaks of sapphire and GaN are not well resolved in figure 5(a). However, from a detailed examination of the peaks, we have concluded that each of these peaks in fact consists of two peaks, hereafter referred to as the main component and the shoulder. First, from an analysis of the relative intensities of the peaks, we immediately notice in figure 5(b) for

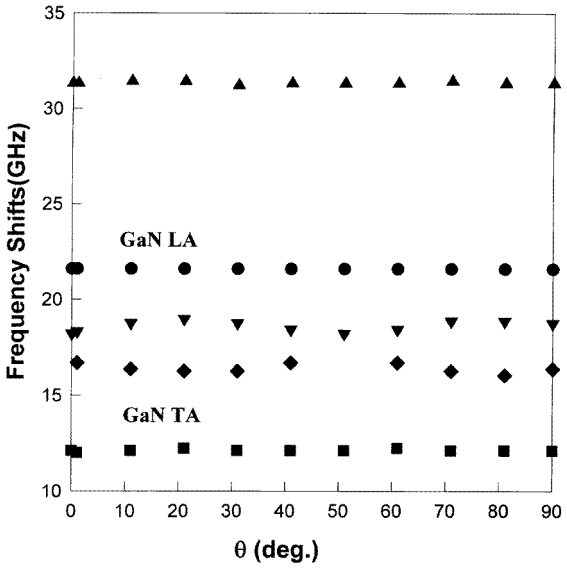

Figure 4. Angular dependence of frequency shifts measured with the rotation of the sample around the *c* axis (the experimental geometry is shown as geometry [A] in figure 1).

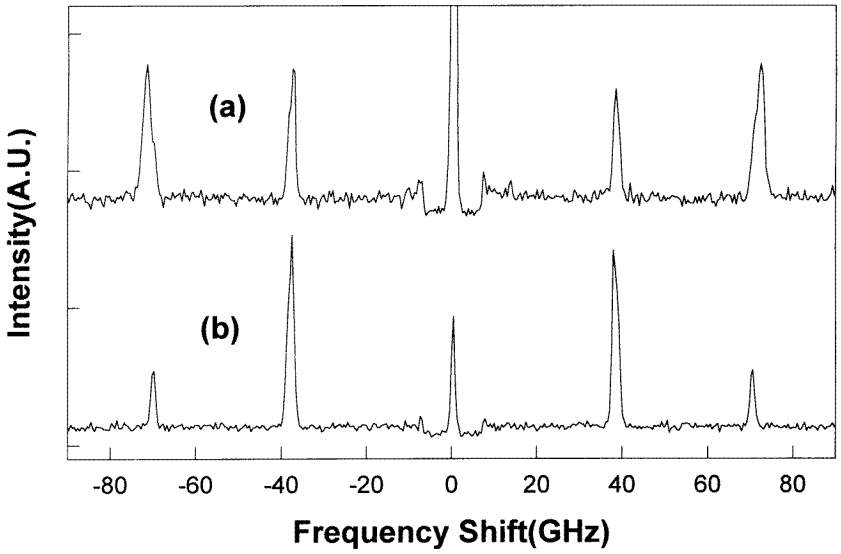

Figure 5. Brillouin scattering spectra of (a) GaN on the sapphire substrate and (b) the sapphire substrate without GaN.

the sapphire substrate that the intensity of the c_{44} depolarized peak (near 38 GHz) is more than twice that of the c_{33} polarized peak (near 70 GHz), but the intensities of the peaks in figure 5(a) are almost the same and, as we have illustrated above, both polarized and depolarized peaks have shoulders near 39 and 70 GHz. It can also be seen that the intensity ratio of the main component of the depolarized peak to the shoulder of the polarized peak

is similar to those of the c_{44} and c_{33} peaks of sapphire. The shoulders in the shape of the peaks in figure 5(a) represent the principal difference from the spectrum in figure 5(b). The peaks in figure 5(a) were accurately fitted with two Lorentzian components and for the peak near 70 GHz a frequency shift of 72.0 GHz was obtained for the main peak and 70.3 GHz for the shoulder. For the peak near 38 GHz, the main peak was found at 37.7 GHz and the shoulder was at 38.6 GHz. The peaks in figure 5(b) were well fitted with one Lorentzian lineshape with frequency shifts of 70.2 GHz and 37.8 GHz, respectively. It is quite evident that the shoulder of the polarized peak corresponds to the c_{33} mode of sapphire and the main component of the depolarized peak corresponds to the c_{44} mode of sapphire. From all these considerations, both peaks in figure 5(a) were concluded to be a superposition of two peaks: c_{33} of sapphire and GaN and c_{44} of sapphire and GaN. The frequency shifts for the c_{33} and c_{44} modes of GaN were obtained from the peak fitting analysis as was described above.

From this analysis, the sound velocities corresponding to the c_{11}, c_{33}, c_{44} and c_{66} modes of GaN were obtained, and the sound velocity corresponding to the c_{12} mode was calculated using the general relation $c_{66} = (c_{11} - c_{12})/2$ for a hexagonal structure. The sound velocity corresponding to the c_{13} mode cannot be measured directly. To obtain its value, we measured the frequency shift for the mixed mode in the scattering geometry when the laser beam was directed onto the sample at an angle of 45° from the c axis, as shown in geometry [C] in figure 1. In this configuration, the quasi-longitudinal mode is expressed as a function of the elastic stiffness c_{13} and also c_{11}, c_{44} and c_{33}, and therefore c_{13} can be calculated in this experiment. It should be noted, however, that this indirect determination of c_{13} leads to a larger uncertainty associated with this elastic constant (table 1).

Table 1. Elastic stiffness constants of GaN obtained by present Brillouin scattering experiments and theoretical values calculated by Azuhata *et al* [16] and Kim *et al* [11].

		Elastic constant (10^{11} dyn cm^{-2})		
Elastic stiffness constant	Sound velocity (m s^{-1})	Experimental this work	Theoretical [16]	[17]
c_{11}	7744	36.5(±0.2)	36.9	39.6
c_{33}	7914	38.1(±0.1)	39.7	47.6
c_{44}	4240	10.9(±0.3)	11.8	9.1
c_{66}	4351	11.5(±0.1)	13.7	12.6
c_{12}	4702	13.5(±0.4)	9.4	14.4
c_{13}	4336	11.4(±1.6)	6.7	6.4

Now, we have obtained all the sound velocities (they are reported in table 1), and the elastic stiffness constants of GaN can be easily calculated from the data. The results are presented in table 1. The experimental elastic constants of GaN in table 1 were obtained using the density $\rho = 6.089$ g cm^{-3} [19]. The refractive indices $n_o = 2.44$ and $n_e = 2.40$ were used to calculate the sound velocity [20], where n_o and n_e are the ordinary and the extraordinary refractive indices, respectively. For sapphire, the density is 4.0 g cm^{-3}, the refractive indices are $n_o = 1.77$ and $n_e = 1.76$, and the elastic constants have been given in [21].

Recently, Azuhata *et al* [16] proposed a new model for calculation of the elastic constants based on the modified version of Keyes's [17] relations and Martin's [18] formula. In this model, the new empirical relations for the elastic constants in the ZB structure are

determined as follows:

$$c_{11}^* = 1.333 + \frac{2.998}{a}$$
$$c_{12}^* = 0.1521a$$
$$c_{44}^* = 0.01235a + 0.1609 + \frac{3.777}{a}$$

where a is the lattice constant, and c_{11}^*, c_{12}^* and c_{44}^* are the reduced elastic stiffnesses defined by Keye as $c_{ij}^* = c_{ij}/c_0$ and $c_0 = e^2/b^4$ (e is the electronic charge and b is the nearest-neighbour distance). The proposed relations reproduce well the elastic stiffness in a number of III–V compounds with ZB structure [16]. Furthermore, the transformation relation between the elastic stiffnesses of the ZB phase and the WZ phase has been derived by Martin [18]. A theoretical analysis based on a combination of the modified version of Keyes's relations and Martin's formula has been performed by Azuhata *et al*; the details of the theoretical model have been previously reported and the theoretical elastic stiffness constants have been calculated for a variety of III–V materials [16]. Now we can compare the experimental elastic constants of GaN with the theoretical values. The calculated elastic stiffness constants are given in table 1, together with the experimental results of the present work. The results of the *ab-initio* calculations of Kim *et al* [11] are also quoted in table 1. The experimental and calculated values of the elastic constants of GaN show good agreement for both the longitudinal c_{11} and c_{33} and the transverse c_{44} modes, and larger differences are observed for other components (table 1). The indirect determination of the parameters which was involved in both experimental work and theoretical modelling of the elastic constants is the main reason for the poor agreement. In particular, c_{13} was obtained from measurements on mixed modes as was discussed above, and c_{12} was calculated from the general relation for a hexagonal structure. The theoretical value of c_{66} was also obtained indirectly in the theoretical models of both Azuhata *et al* and Kim *et al*. As we can see from table 1, the results of the theoretical model of Azuhata *et al* for GaN are in better agreement with the experimental results of this work than are the results of *ab-initio* calculations of Kim *et al* [11] for all elastic constants except c_{12} and c_{66}, but both these parameters involve indirect determination and are less accurate in the comparison. Therefore, the agreement between the experimental elastic constants of GaN obtained in the present study and the theoretical values calculated from the model of Azuhata *et al* [16] is very reasonable. The model has been demonstrated to provide reliable estimates of the elastic constants for many III–V materials, which are not yet available experimentally [16]. It has been pointed out in [16] that the approximations involved in Martin's formula such as the assumption of the ideal WZ structure ($c/a = 1.633$) and an idealized structural transformation model, and neglecting long-range atomic interactions can lead to larger uncertainties in determining theoretical elastic constants in the WZ phase than in the ZB phase. A more rigorous approach to ZB–WZ transformations could be useful.

4. Conclusions

We performed high-resolution Brillouin scattering measurements on the high-quality GaN sample. The elastic constants of GaN were obtained and compared with the theoretical values derived from the recently reported model based on the modified version of Keyes's relations and Martin's formula. Good agreement has been observed for c_{11}, c_{33} and c_{44} elastic constants of WZ-type GaN.

Acknowledgment

This work has been partially supported by Grant-in-Aid 06402009 from the Ministry of Education, Science and Culture, of Japan.

References

[1] Edger J H 1992 *J. Mater. Res.* **7** 235
[2] Strite S and Morkoc H 1992 *J. Vac. Sci. Technol.* B **10** 1237
[3] Asif Khan M, Kuznia J N, Olson D T, van Hove J M, Blasingame M and Reitz L F 1992 *Appl. Phys. Lett.* **60** 2917
[4] Amano H, Tanaka T, Kunii Y, Kato S, Kim S T and Akasaki I 1994 *Appl. Phys. Lett.* **64** 1337
[5] Nakamura S, Harada Y and Senoh M 1991 *Appl. Phys. Lett.* **58** 2021
[6] Nakamura S, Mukai T and Senoh M 1992 *J. Appl. Phys.* **71** 5543
[7] Nakamura S, Mukai T and Senoh M 1994 *Appl. Phys. Lett.* **64** 1687
[8] Nakamura S, Senoh M, Nagahama S, Iwasa N, Yamada T, Matsushita T, Kiyoku H and Sugimoto Y 1996 *Japan. J. Appl. Phys.* **35** L74; 1996 *Japan. J. Appl. Phys.* **35** L217
[9] Kitamura M, Muramatsu S and Harrison W A 1992 *Phys. Rev.* B **46** 1351
[10] San-Guo Shen 1994 *J. Phys.: Condens. Matter* **6** 8733
[11] Kim K, Lambrecht W R L and Segall B 1994 *Phys. Rev.* B **50** 1502
[12] Rodríguez-Hernández P, Gonzalez-Diaz M and Miñoz A 1995 *Phys. Rev.* B **51** 14 705
[13] Azuhata T, Sota T, Suzuki K and Nakamura S 1995 *J. Phys.: Condens. Matter* **7** L129
[14] Sandercock J R 1982 *Light Scattering in Solids III (Topics in Applied Physics 51)* ed M Cardona and G Güntherodt (Berlin: Springer) pp 173–206
[15] Yamaguchi M, Inoue K, Yagi T and Akishige Y 1995 *Phys. Rev. Lett.* **74** 2126
[16] Azuhata T, Sota T and Suzuki K 1996 *J. Phys.: Condens. Matter* **8** 3111
[17] Keyes R W 1962 *J. Appl. Phys.* **33** 3371
[18] Martin R M 1972 *Phys. Rev.* B **6** 4546
[19] Strite S and Morkoc H 1992 *J. Vac. Sci. Technol.* B **10** 1237
[20] Ejder E 1971 *Phys. Status Solidi* a **6** 445
[21] Wachtman J B Jr, Tefft W E, Lam D G and Stinchfield R P 1960 *J. Res. NBS* A **64** 213